Dalton Transactions

Accepted Manuscript

This is an *Accepted Manuscript*, which has been through the Royal Society of Chemistry peer review process and has been accepted for publication.

Accepted Manuscripts are published online shortly after acceptance, before technical editing, formatting and proof reading. Using this free service, authors can make their results available to the community, in citable form, before we publish the edited article. We will replace this *Accepted Manuscript* with the edited and formatted *Advance Article* as soon as it is available.

You can find more information about *Accepted Manuscripts* in the Information for Authors.

Please note that technical editing may introduce minor changes to the text and/or graphics, which may alter content. The journal's standard Terms & Conditions and the Ethical guidelines still apply. In no event shall the Royal Society of Chemistry be held responsible for any errors or omissions in this *Accepted Manuscript* or any consequences arising from the use of any information it contains.

ROYAL SOCIETY OF CHEMISTRY

www.rsc.org/dalton

Cite this: DOI: 10.1039/c0xx00000x

www.rsc.org/xxxxxx

ARTICLE TYPE

Anion templating from a silver(I) dithiophosphate 1D polymer forming discrete cationic and neutral octa- and decanuclear silver(I) clusters

Jian-Hong Liao,[a] Hao-Wei Chang,[a] Yi-Juan Li,[a] Ching-Shiang Fang,[a] Bijay Sarkar,[a] Werner E. van Zyl,*[,b] and C. W. Liu*[,a]

Received (in XXX, XXX) Xth XXXXXXXXX 20XX, Accepted Xth XXXXXXXXX 20XX
DOI: 10.1039/b000000x

We report on a Ag_5 coordination polymer and discrete Ag_8 and Ag_{10} dithiophosphate clusters. The cluster formation and structures was effected by the stoichiometric control of the M:L molar ratios used. The cluster $[Ag_5\{S_2P(O^iPr)_2\}_4]_n(PF_6)_n$, **1**, is a monomeric unit within a coordination polymer formed through the reaction between $[Ag(CH_3CN)_4]PF_6$ and the dithiophosphate ligand, $[S_2P(O^iPr)_2]^-$, used in a M:L molar ratio of 5:4. All other clusters formed in the study are discrete units with encapsulated anions within the metal framework. The clusters $[Ag_8(X)\{S_2P(O^iPr)_2\}_6](PF_6)$ (X = F, **2**, Cl, **3**, Br, **4**) are all cationic and contain monoanionic halogens. The related cluster $[Ag_8(H/D)\{S_2P(O^iPr)_2\}_6](PF_6)$ contains either hydride or deuteride ion, **5** and **5'**, respectively. The cluster $[Ag_8(S)\{S_2P(O^iPr)_2\}_6]$, **6**, is neutral due to the di-anionic nature of the encapsulated sulfide anion. Clusters **2-6** all formed through the reaction between $[Ag(CH_3CN)_4]PF_6$ and $[S_2P(O^iPr)_2]^-$, used in a M:L molar ratio of 8:6 and stirred for 1 hr in THF; thereafter the respective anions (one equiv.) were added *in situ*. The cluster $[Ag_{10}(I)_4\{S_2P(O^iPr)_2\}_6]$, **7**, is also neutral due to the charge balancing of additional metal and halogen. In this case the M:L:X molar ratio was 10:6:4. All new clusters were characterized by ^1H and ^{31}P NMR, elemental analysis and for **1**, **2**, **4-7** by single crystal X-ray diffraction.

Introduction

Negatively charged species play an important role in a range of chemical, biological, medical and environmental processes and as such the area of anion (supramolecular) chemistry has grown tremendously during the past few decades.[1-12] A number of polymetallic cluster and cage complexes have been reported where anions have been shown to control the assembly but such results often stem from serendipitous discovery rather than design strategy.[13-15] A strategic anion template methodology designed to recognize anionic guest species, particularly within competitive aqueous media are current and challenging research endeavours.[12] Such systems typically rely on classic organic rotaxane and catenane receptors that contain unique anion binding cavity domains and show high levels of anion selectivity in aqueous media.

[a]*Department of Chemistry, National Dong Hwa University, Hualien, Taiwan 97401, R.O.C. Fax: +886-3-8633570, E-mail: chenwei@mail.ndhu.edu.tw*
[b]*School of Chemistry and Physics, University of KwaZulu-Natal, Westville Campus, Private Bag X54001, Durban, 4000, South Africa . E-mail: vanzylw@ukzn.ac.za*
†Electronic Supplementary Information (ESI) available: Solution NMR spectra. The structures reported herein have been deposited at the Cambridge Crystallographic Data Centre, CCDC #977326-977331.

Additionally, redox-active ferrocene and photo-active transition-metal complexes within host structures enables such materials to selectively sense anions by electrochemical and optical means.

Coordination polymeric[16] and cluster[17] compounds formed by silver(I) with sulfur donor ligands are known to exhibit a great variety of structural motifs. The first reported examples entrapped the sulfide anion, albeit not by design.[18] Modification of complexes from an extended network (coordination polymer) to a discrete cluster in the presence of an anion is rare.[19]

We started to explore the chemistry of Ag_8 and Ag_{10} diselenophosphate clusters more than a decade ago and demonstrated the effective encapsulation of selenide and halide within the cluster.[20] More recently, we communicated the template synthesis of Ag_8 dithiophosphate (dtp) clusters and the encapsulation of a number of anions[21] including the novel μ_9-iodide within a tricapped trigonal-prismatic geometry.[22] We propose that these products are formed through *designed anionic templating* because i) the M:L:X ratio used corresponds with the stoichiometric ratio in the final product formed in good yield, and ii) in our hands we cannot form and isolate the un-encapsulated species $[Ag_8\{S_2P(OR)_2\}_6]^{2+}$ suggesting it is derived from the readily prepared and stable lower nuclearity polymeric cluster $[Ag_5\{S_2P(OR)_2\}_4]^+$ reported herein.

Dalton Transactions Accepted Manuscript

Experimental

Materials and measurements

The organic solvents acetone, dichloromethane, and tetrahydrofuran were purchased from Mallinckrodt Chemicals, and purified by standard procedures.[23] Other reagent grade chemicals were purchased from Aldrich. All the reactions were carried out in oven-dried Schlenk glassware under an inert atmosphere of nitrogen. Elemental analyses were recorded with a Heraeus VarioEL-III CNH analyzer. Multinuclear (^{1}H, ^{31}P) NMR spectra were recorded with a Bruker Avance DPX300 FT-NMR spectrometer operating at 300.130 and 121.495 MHz for recording ^{1}H and ^{31}P NMR spectra, respectively. The ^{31}P{^{1}H} NMR spectra were referenced externally against 85% H_3PO_4 (δ = 0 ppm). ^{19}F NMR spectra were recorded on a Bruker Avance II 400 spectrometer operating at 376.5 MHz, referenced against neat $CFCl_3$ (δ = 0 ppm). A ^{109}Ag{^{1}H} NMR spectrum was recorded on a Bruker 600 UltraShield spectrometer operating at 28.0 MHz, referenced against a 3M aqueous solution of $AgNO_3$ (δ = 0 ppm). The chemical shift (δ) and coupling constant (J) are reported in parts per million and hertz, respectively. The NMR spectra were recorded at ambient temperature. $(NH_4)[S_2P(O^iPr)_2]$ was prepared by the method reported by Wystrach[24] whereas $(NH_4)[S_2P(OEt)_2]$ was obtained from Aldrich. $[Ag(CH_3CN)_4](PF_6)$ was synthesized following the literature procedure.[25]

Synthesis

$[Ag_5\{S_2P(O^iPr)_2\}_4]_n(PF_6)_n$, 1.

$[Ag(CH_3CN)_4](PF_6)$ (0.451 g, 1.08 mmol) and $NH_4[S_2P(O^iPr)_2]$ (0.200 g, 0.86 mmol) were added to a 100 mL flask, followed by 20 mL of THF. The colorless solution was stirred at -20 ^{o}C for 1 h and then filtered to remove solids. The filtrate was evaporated to dryness under a vacuum. The residual was dissolved in CH_2Cl_2 (30 mL) and washed with deionized water (20 mL x 3). The CH_2Cl_2 layer was then isolated and dried under vacuum. The white solid was washed with diethyl ether and methanol to remove any NH_4PF_6 formed during the reaction and dried under a vacuum to obtain $[Ag_5\{S_2P(O^iPr)_2\}_4]_n(PF_6)_n$ as a light-yellow powder. Yield: 0.286 g (86 %). Mp. 156 ^{o}C. Anal. calcd for $Ag_5H_{56}C_{24}O_8P_5F_6S_8{\cdot}2H_2O$: C, 18.32; H, 3.84. Found: C, 18.13; H, 4.08. ^{1}H NMR ($CDCl_3$): 1.42 (d, $^3J_{HH}$ = 6.1 Hz, 48 H, CH_3), 4.84 (m, 8 H, CH); ^{31}P NMR ($CDCl_3$): 103.2, -143.0 (septet, J_{PF} = 712 Hz, PF_6).

$[Ag_8(\mu_8\text{-F})\{S_2P(O^iPr)_2\}_6](PF_6)$, 2.

$[Ag(CH_3CN)_4](PF_6)$ (0.534 g, 1.28 mmol) and $NH_4[S_2P(O^iPr)_2]$ (0.222 g, 0.96 mmol) were charged in a 100 mL flask and 20 mL THF was added. The solution was stirred at -20 ^{o}C for 1 h and then tetrabutylammonium fluoride (0.04, 0.16 mmol) was added to the flask and stirring was continued for 12h. The mixture was filtered to remove solids. The filtrate was evaporated to dryness under a vacuum. The residual was dissolved in CH_2Cl_2 (30 mL) and washed with deionized water (20 mL x 3). The CH_2Cl_2 layer was then isolated and dried under vacuum. The solid was washed with diethyl ether and methanol to remove any ammonium salt formed during the reaction and dried under a vacuum to obtain $[Ag_8(F)\{S_2P(O^iPr)_2\}_6](PF_6)$ as a light brown powder. Yield: 0.230 g (62.3%). Mp. 159 ^{o}C. Anal. calcd for $C_{36}H_{84}Ag_8F_7O_{12}P_7S_{12}$: C 18.75; H 3.67; Found: C, 18.72; H, 3.67 %. ^{1}H NMR ($CDCl_3$): 1.37 (d, $^3J_{HH}$ = 6.2 Hz, 72H, CH_3), 4.91 (m, 12H, CH); ^{31}P{^{1}H} NMR ($CDCl_3$): 106.4, -143.0 (septet, J_{PF} = 712 Hz, PF_6). ^{19}F NMR ($CDCl_3$): -166.6 (nonet, J_{FAg} = 42.6 Hz, Ag_8F), -74.3 (d, J_{PF} = 713 Hz, PF_6).

$[Ag_8(\mu_8\text{-Cl})\{S_2P(O^iPr)_2\}_6](PF_6)$, 3.

$[Ag(CH_3CN)_4](PF_6)$ (0.534 g, 1.28 mmol) and $NH_4[S_2P(O^iPr)_2]$ (0.222 g, 0.96 mmol) were charged in a 100 mL flask and 20 mL THF was added. The solution was stirred at -20 ^{o}C for 1 h and then benzyltriethylammonium chloride (0.037 g, 0.16 mmol) was added to the flask and stirring was continued for 3h. The residual was dissolved in CH_2Cl_2 (30 mL) and washed with deionized water (20 mL x 3). The CH_2Cl_2 layer was then isolated and dried under vacuum. The white solid was washed with diethyl ether and methanol to remove any NH_4PF_6 formed during the reaction and dried under a vacuum to obtain $[Ag_8(Cl)\{S_2P(O^iPr)_2\}_6](PF_6)$ as a white powder. Yield: 0.264 g (71 %). Mp. 177 ^{o}C. Anal. calcd for $C_{36}H_{84}Ag_8ClF_6O_{12}P_7S_{12}$: C, 18.61; H, 3.64. Found: C, 18.80; H, 3.67 %. ^{1}H NMR ($CDCl_3$): 1.40 (d, $^3J_{HH}$ = 6.2 Hz, 72H, CH_3), 4.82 (m, 12H, CH); ^{31}P{^{1}H} NMR ($CDCl_3$): 105.8, -143.0 (septet, J_{PF} = 712 Hz, PF_6).

$[Ag_8(\mu_8\text{-Br})\{S_2P(O^iPr)_2\}_6](PF_6)$, 4.

Complex **4** was synthesized in a similar manner as described for **2** by using PPh_4Br (0.067 g, 0.16 mmol). Yield: 0.239 g (63%). Mp. 182 ^{o}C. Anal. calcd for $C_{36}H_{84}Ag_8BrF_6O_{12}P_7S_{12}$: C 18.26; H 3.58,. Found: C, 18.23; H, 3.47 %. ^{1}H NMR ($CDCl_3$): 1.40 (d, $^3J_{HH}$ = 6.6 Hz, 72H, CH_3), 4.82 (m, 12H, CH).^{31}P{^{1}H} NMR ($CDCl_3$): 106.4, -143.0 (septet, J_{PF} = 712 Hz, PF_6).

$[Ag_8(\mu_4\text{-H})\{S_2P(O^iPr)_2\}_6](PF_6)$, 5.

$[Ag(CH_3CN)_4](PF_6)$ (0.534 g, 1.28 mmol) and $NH_4[S_2P(O^iPr)_2]$ (0.222 g, 0.96 mmol) were charged in a 100 mL flask and 20 mL THF was added. The solution was stirred at -20 ^{o}C for 1 h and then $NaBH_4$ (0.006 g, 0.16 mmol) was added to the solution and stirred for a further 30 min. The mixture was filtered to remove all solids. The filtrate was evaporated to dryness under a vacuum. The solid was recrystallized from CH_2Cl_2 and dried under a vacuum to obtain $[Ag_8(H)\{S_2P(O^iPr)_2\}_6](PF_6)$, as a light-brown powder. Yield: 0.216 g (59%). Mp. 143 ^{o}C. Anal. calcd for $C_{36}H_{85}Ag_8F_6O_{12}P_7S_{12}$: C 18.89; H 3.74. Found: C, 19.21; H, 3.72 %. ^{1}H NMR ($CDCl_3$): 1.40 (d, $^3J_{HH}$ = 6.2 Hz, 72H, CH_3), 4.79 (m, 12H, CH), 5.90 (nonet, J_{HAg} = 33.3 Hz, 1H, μ_4-H); ^{31}P{^{1}H} NMR ($CDCl_3$): 105.5, -143.0 (septet, J_{PF} = 712 Hz, PF_6). ^{109}Ag NMR ($CDCl_3$): 967.7 (d, $^1J_{AgH}$ = 44.0 Hz).

$[Ag_8(D)\{S_2P(O^iPr)_2\}_6](PF_6)$, 5'.

Complex **5'** was synthesized in a similar manner as described for **5** using $NaBD_4$ instead of $NaBH_4$. Yield: 0.187 g (51%). Mp. 141 ^{o}C. Anal. calcd for $C_{36}H_{84}DAg_8F_6O_{12}P_7S_{12}$: C 18.88; H 3.79,. Found: C, 19.06; H, 3.60 %. ^{1}H NMR ($CDCl_3$): 1.40 (d, $^3J_{HH}$ = 6.2 Hz, 72H, CH_3), 4.80 (m, 12H, CH). ^{2}H NMR ($CHCl_3$): 6.05. ^{31}P{^{1}H} NMR ($CDCl_3$): 105.7, -143.0 (septet, J_{PF} = 713 Hz, PF_6).

Dalton Transactions Accepted Manuscript

This journal is © The Royal Society of Chemistry [year]

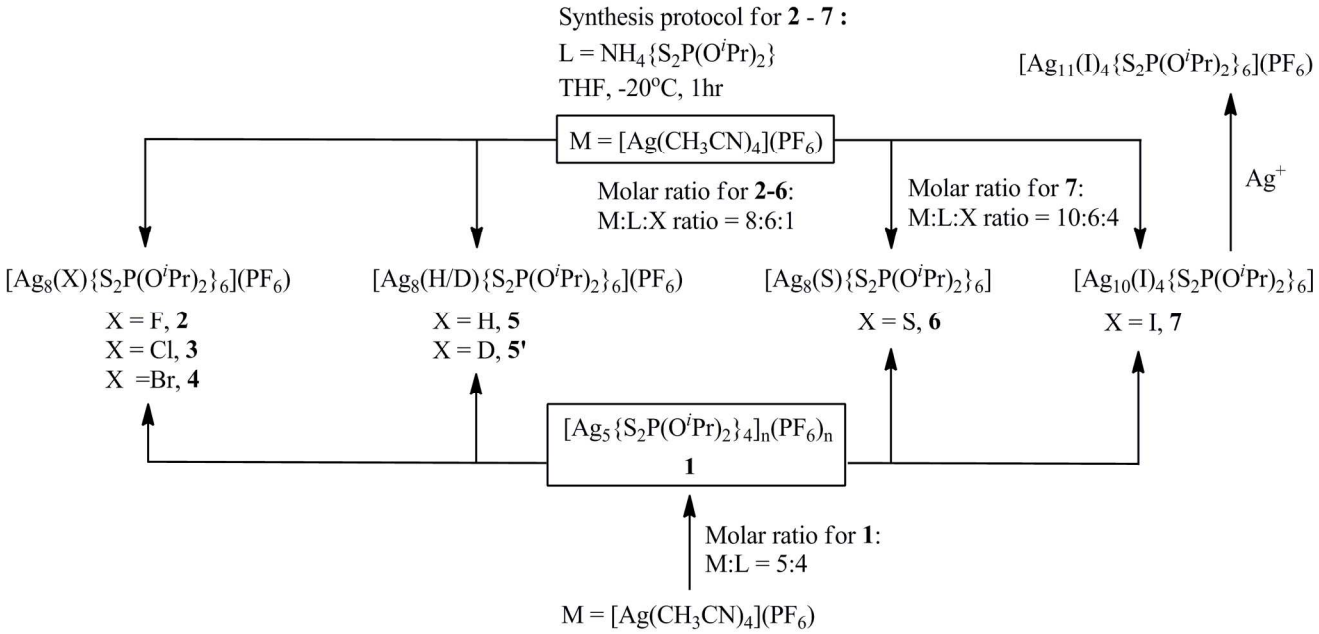

Scheme 1 Synthesis methodology followed in the present study. Lower reactions form complexes **2-7** from the *in-situ* prepared $[Ag_5\{S_2P(O^iPr)_2\}_4]_n(PF_6)_n$ coordination polymer, followed by addition of suitable anionic (X) template in correct stoichiometric ratio. Upper reactions start with $[Ag(CH_3CN)_4]PF_6$ and form complexes **2-7** through strict control of the M:L:X ratios.

$[Ag_8(\mu_8\text{-}S)\{S_2P(O^iPr)_2\}_6]$, 6.

$[Ag(CH_3CN)_4]PF_6$ (0.534 g, 1.28 mmol) and $NH_4[S_2P(O^iPr)_2]$ (0.222 g, 0.96 mmol) were charged in a 100 mL Schlenk flask and a 20 mL THF solution was prepared that was stirred at -20 ℃ for 1 h. To the solution solid Na_2S (0.017 g, 0.16 mmol) was added, and the filtrate was evaporated to dryness under a vacuum. The solid was washed with deionized water to remove any NH_4PF_6 formed during the reaction and dried under a vacuum to obtain $[Ag_8(S)\{S_2P(O^iPr)_2\}_6]$ as a yellow powder. Yield: 0.094 g (27%). Mp. 151 °C. Anal. calcd for $C_{36}H_{84}Ag_8O_{12}P_6S_{13}$: C 19.88; H 3.89. Found: C 19.33,; H 3.61, %. ^{1}H NMR (acetone-d_6): 1.41 (d, $^3J_{HH}$ = 6.9 Hz, 72H, C*H*$_3$), 4.92 (m, 12H, C*H*). ^{31}P{^{1}H} NMR (acetone-d_6): 104.1.

$[Ag_{10}(\mu_9\text{-}I)(\mu_3\text{-}I)_3\{S_2P(O^iPr)_2\}_6]$, 7.

Solid $[Ag(CH_3CN)_4](PF_6)$ (0.300 g, 0.72 mmol) and $(NH_4)[S_2P(O^iPr)_2]$ (0.100 g, 0.43 mmol) were added to a flame-dried Schlenk tube and a 20 mL methanol solution were prepared at ambient temperature and stirred for 1 h under nitrogen. Bu_4NI (0.107 g, 0.29 mmol) was added to the yellow solution and stirred for 1 h. The yellow precipitate was collected by filtration and washed with deionized water and diethyl ether to obtain a light yellow powder of $[Ag_{10}(I)_4\{S_2P(O^iPr)_2\}_6](PF_6)$. Yield: 0.167 g (80.7%). Mp. 186 °C. Anal. calcd for $C_{36}H_{84}Ag_{10}I_4O_{12}P_6S_{12}{\cdot}CH_3OH$: C 15.33; H 3.06. Found: C 15.24,; H 3.42. ^{1}H NMR ($CDCl_3$): 1.36 (d, $^3J_{HH}$ = 6.9 Hz, 72H, C*H*$_3$), 4.92 (m, 12H, C*H*). ^{31}P{^{1}H} NMR ($CDCl_3$): 105.9.

X-ray structure determination

Crystals were mounted on glass fibers with epoxy resin, and all geometric and intensity data were collected on a Bruker APEXII CCD diffractometer using graphite monochromated Mo-Kα radiation (λ = 0.71073 Å). Data reduction was carried out with *SAINT-Plus* software.[26] An empirical absorption correction was applied using the *SADABS* program.[27] Structures were solved by direct methods and refined by full-matrix least-squares on F^2 using the *SHELXTL* software package,[28] incorporated in *SHELXTL*/PC version 5.10.[29] Crystal data and selected bond lengths and angles for **1, 2, 4**–**7** are summarized in Tables **1**–**5**.

Results and discussion

Synthesis

The synthesis methods followed for the formation of clusters **1-7** is summarized in Scheme 1. The complexes **2-7** can be prepared in one of two ways: i) generation of complex **1** *in-situ*, followed by addition of appropriate anion, or ii) generate clusters **2-7** from $[Ag(CH_3CN)_4](PF_6)$ by allowing strict control of the relevant metal:ligand:anion (M:L:X) molar ratios. We focused on the latter methodology in the experimental and discussion sections. Complex **1** was prepared from the reaction between the THF-soluble silver(I) precursor $[Ag(CH_3CN)_4](PF_6)$ together with the ammonium salt of the isopropyl derivate of dithiophosphate in a M:L molar ratio of 5:4. The R = ^{i}Pr ligand derivate was used throughout the study. The colorless solution was stirred at -20 °C for 1 h and then filtered. Following work-up, complex **1** was obtained as a light-yellow powder in a good yield (>85%). Complexes **2-7** were prepared in a much similar manner. The silver(I) precursor $[Ag(CH_3CN)_4](PF_6)$ was added to the salt $NH_4[S_2P(O^iPr)_2]$ and the THF solution stirred at -20 °C for 1 h. This was followed by addition of appropriate anion source, ie

Dalton Transactions Accepted Manuscript

tetrabutylammonium fluoride for **2**, benzyltriethylammonium chloride for **3**, PPh_4Br for **4**, $NaBH_4$ for **5**, Na_2S for **6**, and Bu_4NI for **7**. Importantly, the anions were added in a M:L:X ratio of 8:6:1 for clusters **2-6**, and in a 10:6:4 ratio for **7**. The dianionic nature of the sulfide in **6** and the difference in ratios used for **7**, respectively, results in those clusters being neutral. The crude product was typically co-precipitated with the salt byproduct through removal of the solvent and then extracted by washing the ammonium or sodium salt away with deionized water. Complexes **2-7** were all obtained in reasonable yields except **6** (27%).

Solution NMR

Complexes **1-7** were characterized by ^{1}H and $^{31}P\{^{1}H\}$ solution NMR, and additionally ^{19}F and ^{109}Ag NMR was used where appropriate. Each of the silver(I) clusters prepared, exhibits only a single resonance in the ^{31}P NMR spectrum suggesting all the dtp ligands remain equivalent in solution. The ^{1}H NMR spectra of compounds **1-7** exhibit peaks corresponding to one set of methine proton (multiplet) and one set of methyl proton (doublet) from the isopropyl moieties. This phenomenon suggested that all the dtp ligands in the complexes are equivalent in solution. In addition, compound **5** also exhibited the hydride resonance at 5.9 ppm (Figure S11). The hydride peak for **5** could be observed as a nonet ($^{1}J_{107Ag,\ 109Ag\text{-}H}$ = 33.3 Hz) due to the coupling of hydride nuclei with eight Ag nuclei. On the other hand, **5'** exhibited a broad peak at 6.05 ppm in the ^{2}H NMR spectrum, originating from the entrapped deuteride (Figure S16). A similar coupling pattern like **5** was not identified due to both the much smaller magnetogyric ratio of deuterium (γ_H/γ_D= 6.514) and the poor spectral resolution. We further carried out a ^{109}Ag NMR experiment to confirm the magnetic interaction of entrapped hydride and Ag(I) nuclei and observed a doublet at 967.7 ppm (J_{AgH} = 44 Hz) (Figure S12), which suggests magnetic equivalence in solution of all eight Ag nuclei. ^{19}F NMR of **2** exhibits the encapsulated fluoride at -166.6 ppm, which displays a poor-resolved nonet peak, together with the hexafluorophosphate resonance at -74.3 ppm (Figure S5).

X-ray crystal structures

Complexes **1**, **2**, **4-7** were characterized by single crystal X-ray crystallography. Complex **1** crystallizes in monoclinic space group C2/c. Selected bond lengths and angles are presented in Table 1. A perspective view of cluster **1** is shown in Fig. 1. The X-ray structure reveals that repeating units of the 1D polymeric species contains five Ag atoms bridged by S atoms of four dithiophosphate ligands in a tetrametallic-tetraconnective (μ_2, μ_2) binding mode. The Ag_5 atom of each repeating unit is connected to two bridging S atoms (S2 and S3) from two independent ligands of the neighboring unit. Inspection reveals the atoms Ag1, Ag2, Ag3 and Ag4 constitute a tetrahedral structure with the edge lengths in the range of 3.102(2)–3.290(1) Å, all of which are less than twice the sum of the van der Waals radii of Ag (3.4 Å)[30] and Ag5 is situated at 3.070(1) and 4.048(1) Å from Ag3 and Ag1, respectively. Each of the Ag atoms forming the tetrahedron (Ag1-Ag4) is coordinated to three bridging S atoms from three dtp ligands in a planar-trigonal manner, but Ag5 is coordinated to a total of four S atoms in an approximately tetrahedral manner. The average S···S intraligand bite distance is 3.443(3) Å. Ag-S bond lengths 2.444(3)-2.648(4) Å are in their normal range which is comparable to $[Ag(S_2P(O^iPr)_2)]_6$.[17c]

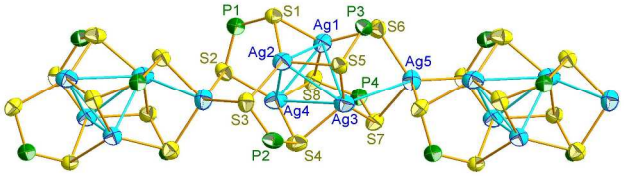

Fig. 1 Thermal ellipsoid drawing (50% probability) of cluster $[Ag_5\{S_2P(O^iPr)_2\}_4]_n(PF_6)_n$, **1**. Only the framework Ag/S/P atoms are shown for clarity.

Table 1 Selected bond distances (Å) and angles (deg) for **1** and **2** with e.s.d.s. in parentheses.

Complex **1**			
Ag(1)–S(1)	2.521(3)	Ag(5)–S(6)	2.582(3)
Ag(1)–S(6)	2.502(2)	Ag(5)–S(7)	2.649(3)
Ag(1)–S(8)	2.493(3)	P(1)–S(1)	2.009(3)
Ag(2)–S(1)	2.481(2)	P(1)–S(2)	1.999(4)
Ag(2)–S(3)	2.486(2)	P(2)–S(3)	1.993(4)
Ag(2)–S(5)	2.559(2)	P(2)–S(4)	2.010(3)
Ag(3)–S(4)	2.591(3)	P(3)–S(5)	2.017(3)
Ag(3)–S(5)	2.521(3)	P(3)–S(6)	1.996(3)
Ag(3)–S(7)	2.573(3)	P(4)–S(7)	1.988(2)
Ag(4)–S(2)	2.516(2)	P(4)–S(8)	2.024(3)
Ag(4)–S(4)	2.442(2)	S(1)–P(1)–S(2)	119.9(1)
Ag(4)–S(8)	2.581(2)	S(3)–P(2)–S(4)	119.0(2)
Ag(5)–S(2)	2.637(2)	S(5)–P(3)–S(6)	116.8(1)
Ag(5)–S(3)	2.544(2)	S(7)–P(4)–S(8)	117.8(1)
Complex **2**			
Ag(1)–S(1)	2.509(1)	P(1)–S(2)	1.989(2)
Ag(1)–S(3)	2.511(1)	P(2)–S(6)	1.993(1)
Ag(1)–S(6)	2.514(1)	P(2)–S(4)	2.009(1)
Ag(2)–S(1)	2.502(1)	P(3)–S(5)	2.007(1)
Ag(2)–S(4)	2.508(1)	P(3)–S(3)	2.005(2)
Ag(2)–S(5)	2.499(1)	F(1)–Ag(1)	2.6634(4)
Ag(3)–S(2)	2.504(1)	F(1)–Ag(2)	2.7898(5)
Ag(3)–S(5)	2.497(1)	F(1)–Ag(3)	2.7276(4)
Ag(3)–S(6)	2.501(1)	F(1)–Ag(4)	2.7270(5)
Ag(4)–S(2)	2.493(1)	S(1)–P(1)–S(2)	121.95(8)
Ag(4)–S(3)	2.483(1)	S(6)–P(2)–S(4)	122.25(6)
Ag(4)–S(4)	2.485(1)	S(5)–P(3)–S(3)	121.64(7)
P(1)–S(1)	2.008(2)		

Complex **2** also crystallize in the monoclinic space group C2/c. Selected bond lengths and angles are presented in Table 1. A perspective view of complex **2** is shown in Fig. 2. The X-ray structure reveals that the cluster contains a slightly distorted cubic Ag_8 core with an entrapped fluoride. Each of the faces of the Ag_8 cube is capped by a dtp ligand in a tetrametallic-tetraconnective (μ_2, μ_2) coordination pattern. The cluster contains an inversion center and each Ag atom is trigonally coordinated to three S atoms from three independent ligands. Twelve sulfur atoms from six ligands are located on the vertices of a slightly distorted icosahedron in an idealized T_h point group symmetry. Thus six P atoms and twelve S atoms of the ligands are symmetry-related and this is also reflected by the ^{31}P NMR studies (see above). The ligand "bite" distances of 3.495(2) ~ 3.505(2) Å and Ag-S bond lengths are in the range 2.483(1) to 2.514(1) Å. The Ag···Ag edge distances are in the range 3.1132(5) to 3.1771(5) Å, and suggest the presence of argentophilic interactions whilst the Ag_8 cube is the more regular (least distorted) in this series. The average Ag-F

Dalton Transactions Accepted Manuscript

This journal is © The Royal Society of Chemistry [year]

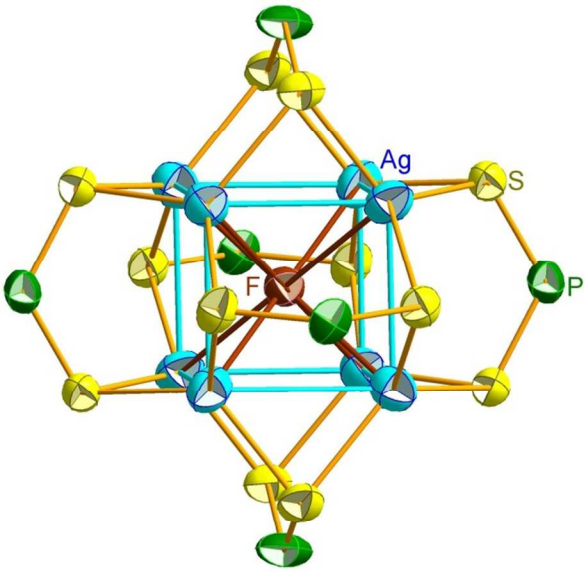

Fig. 2 Thermal ellipsoid drawing (50% probability) of the cluster $[Ag_8(\mu_8\text{-}F)\{S_2P(O^iPr)_2\}_6](PF_6)$, **2.** Only the framework Ag/S/P/F atoms are shown for clarity.

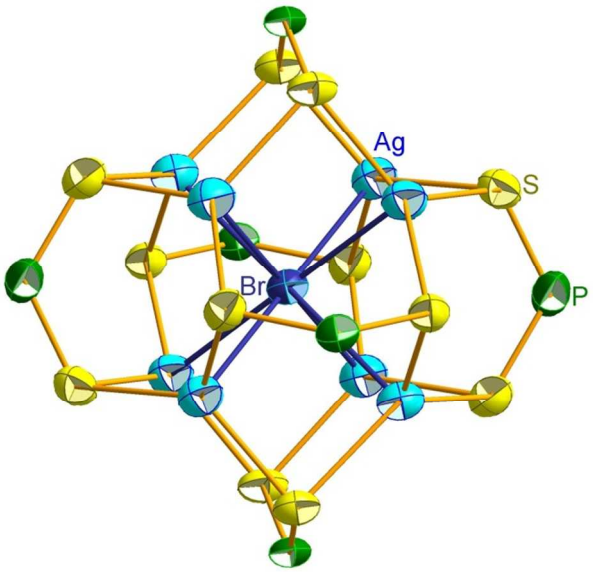

Fig. 3 Thermal ellipsoid drawing (50% probability) of **[**$Ag_8(\mu_8\text{-}Br)\{S_2P(O^iPr)_2\}_6](PF_6)$, **4**. Only the framework Ag/S/P/Br atoms are shown for clarity.

distance is 2.727(1) Å. For the corresponding compound, $[Ag_8(F)\{S_2P(OEt)_2\}_6]PF_6$,[21] the Ag_8 skeleton revealed more distortion away from a regular cube where its face diagonal become the edges of a tetrahedron in a tetrahedral contraction.[31] Considering the Ag_8 skeleton in **2** as an ideal cube, we assumed the Ag_8 cube has all the edges equal to a length of 3.149 Å which is averaged from within the cube. With such an edge length, the face diagonal can be calculated to be 4.453 (3.149 x √2) Å, which is about 7.2 % larger than that of the average edge length (4.133 Å) of the tetrahedron observed in $[Ag_8(F)\{S_2P(OEt)_2\}_6]PF_6$. In other words, a fluoride anion manifested 7.2 % tetrahedral contraction in the ethyl homolog whereas for isopropyl it remains in a cube. Cationic clusters of the type $[Ag_{14}(C{\equiv}C^tBu)_{12}X]^+$ with entrapped X = Br, Cl, F anions and each containing an Ag_6 octahedron have been reported.[32] Each of the triangular faces capped by 8 Ag atoms showed an overall shrinking of the Ag cage dimension on reducing the size of encapsulated anion from chloride to smaller fluoride. The shortest Ag···Ag distances in $[Ag_{14}(C{\equiv}C^tBu)_{12}F]^+$ was between 2.898(2) and 2.920(2) Å which are ~0.06 Å shorter than for $[Ag_{14}(C{\equiv}C^tBu)_{12}Cl]^+$ and indicates the amount of shrinkage of the metallic core. The Ag-F bond lengths are in the range 2.949(2)-3.292(2) Å and much longer than the fluoride–centered cluster **2** described in the present study, and indicative of a stronger Ag···F interaction.

The crystallographic data of complex **3** was not obtained, however, it revealed similar resonance to complex **2**–**5** in the ^{31}P indicates that ligands have a similar coordination environment (μ_2, μ_2) in solution. In the previous study, $[Ag_8(F)\{S_2P(OEt)_2\}_6]PF_6$ and $[Ag_8(Cl)\{S_2P(OEt)_2\}_6]PF_6$ displayed not only similar resonances in ^{31}P NMR spectra but also in the structural framework.[21] Considering the template effect during the reaction, $[Ag_5\{S_2P(O^iPr)_2\}_4]_n(PF_6)_n$ can be transformed into $[Ag_8(X)\{S_2P(OEt)_2\}_6]PF_6$ (X = halide anion) in the presence of halide anion. Against this background, we suggest that the molecular formula of complex **3** is $[Ag_8(Cl)\{S_2P(O^iPr)_2\}_6]PF_6$ in the absence of an actual structural study.

Complex **4** crystallized in the triclinic space group $P\bar{1}$. Selected bond lengths and angles are presented in Table 3. A perspective view of cluster **4** is shown in Fig. 3. The X-ray structure reveals that the cluster contains a slightly distorted cubic Ag_8 core with an entrapped bromide. Each of the faces of the Ag_8 cube is capped by a dtp ligand in a tetrametallic-tetraconnective (μ_2, μ_2) coordination pattern. The cluster contains an inversion center andeach Ag atom is trigonally coordinated to three S atoms from three independent ligands. Twelve sulfur atoms from six ligands lie on the faces of the Ag_8 cube, maintaining an idealized T_h point group symmetry. Thus six P atoms and twelve S atoms of the ligands are symmetry-related and this is also reflected by the ^{31}P NMR studies (see above). The ligand "bite" distances of 3.517(3) ~ 3.534(3) Å and Ag–S bond lengths are in the range 2.511(3) to 2.552(2) Å. The Ag···Ag edge distances are in the range 3.323(1) to 3.442(1) Å (avg. in 3.380 Å).

Such a distance indicates a very weak argentophilic interaction, yet the structure remains intact, presumably through the stabilizing effect of the dtp ligands and further supported by the interaction between Ag atoms and the encapsulated anion. The average Ag–Br distance is 2.927 Å. Compared with $[Ag_8(Br)\{Se_2P(OR)_2\}_6]PF_6$ (R = Et, Pr),[20c] Ag···Ag and Ag–Br distances are in similar range. Neither the dithiophosphato nor diselenophosphato ligand bring any change to the Ag_8Br core parameters. Furthermore, the Ag_8 cube expanded slightly due to the size effect of the encapsulated bromide anion. As a result, the ligand "bite" distances and the edge of Ag_8 cube are longer than those in complex **2**.

Complex **5** crystallize in the triclinic space group $P\bar{1}$. Selected bond lengths and angles are presented in Table 3. A perspective view of cluster **5** is shown in Fig. 4 and a different perspective showing only the Ag_8H core is shown in Fig. 5. The cluster involving the ethyl homologue of the dithiophosphato ligand, which crystallizes in the trigonal $R\bar{3}c$ space group, is the only reported hydride-encapsulated octanuclear metallic cluster in which the tetracapped tetrahedral silver skeleton is not

Dalton Transactions Accepted Manuscript

Table 2 X-ray crystallographic data for clusters **1, 2, 4-7**.

	1	**2**	**4**	**5**	**6**	**7**
Formula	$C_{24}H_{56}Ag_5F_6O_8P_5S_8$	$C_{36}H_{84}Ag_8F_7O_{12}P_7S_{12}$	$C_{36}H_{84}Ag_8BrF_6O_{12}P_7S_{12}$	$C_{36}H_{85}Ag_8F_6O_{12}P_7S_{12}$	$C_{36}H_{84}Ag_8O_{12}P_6S_{13}$	$C_{36}H_{84}Ag_{10}I_4O_{12}P_6S_{12}$
Fw	1545.37	2306.50	2367.41	2288.51	2174.59	2865.87
Space group	*C*2/*c*	*C*2/*c*	$P\bar{1}$	*C*2/*c*	$P\bar{1}$	*P*2(1)/*n*
a, Å	35.148(3)	24.1642(10)	12.870(4)	24.1617(8)	12.8486(12)	14.5923(10)
b, Å	16.7802(16)	13.1505(6)	13.066(2)	13.1118(5)	12.9911(6)	23.5026(15)
c, Å	23.300(2)	24.9918(11)	13.778(2)	24.9456(9)	13.7516(6)	24.2656(16)
α, deg.	90	90	117.176(3)	90	117.1860(10)	90
β, deg.	127.931(2)	92.3660(10)	99.416(5)	92.3010(10)	99.3420(10)	92.122(2)
γ, deg.	90	90	95.281(5)	90	95.4300(10)	90
V, Å^3	10839.1(18)	7934.9(6)	1996.3(8)	7896.5(5)	1977.1(2)	8316.4(10)
Z	8	4	1	4	1	4
ρ_{calcd}, g cm^{-3}	1.884	1.931	1.969	1.925	1.826	2.289
μ, mm^{-1}	2.287	2.447	2.930	2.457	2.444	4.243
T, K	296(2)	296(2)	296(2)	296(2)	296(2)	296(2)
θ_{max}, deg.	25.00	26.42	25.00	25.00	25.00	25.00
Completeness, %	99.8	99.7	97.9	100.0	98.6	100.0
Reflections collected	30306	24740	11357	34095	13120	73589
Independent reflections	9527 (R_{int}= 0.0461)	8147 (R_{int} = 0.0276)	6896 (R_{int} = 0.0373)	6961 (R_{int}= 0.0389)	6878 (R_{int} = 0.0227)	14642 (R_{int}= 0.0329)
*R*1[a], *wR*2[b] [I>2σ(I)]	0.0481, 0.1242	0.0338, 0.0834	0.0631, 0.1886	0.0499, 0.1292	0.0358, 0.1007	0.0331, 0.0781
*R*1[a], *wR*2[b] (all data)	0.0775, 0.1378	0.0461, 0.0907	0.0696, 0.1981	0.0660, 0.1437	0.0462, 0.1062	0.0449, 0.0855
Goodness of fit	0.978	1.015	1.033	1.073	1.076	1.016
Largest diff. peak and hole, e/Å^3	1.097 and -0.760	0.668 and -0.821	1.457 and -1.659	3.670 and -0.584	0.833 and -0.963	2.292 and -1.734

[a] $R1 = \Sigma \left| |F_o| - |F_c| \right| / \Sigma |F_o|$. [b] $wR2 = \{\Sigma[w(F_o^2 - F_c^2)^2] / \Sigma[w(F_o^2)^2]\}^{1/2}$.

Dalton Transactions Accepted Manuscript

This journal is © The Royal Society of Chemistry [year]

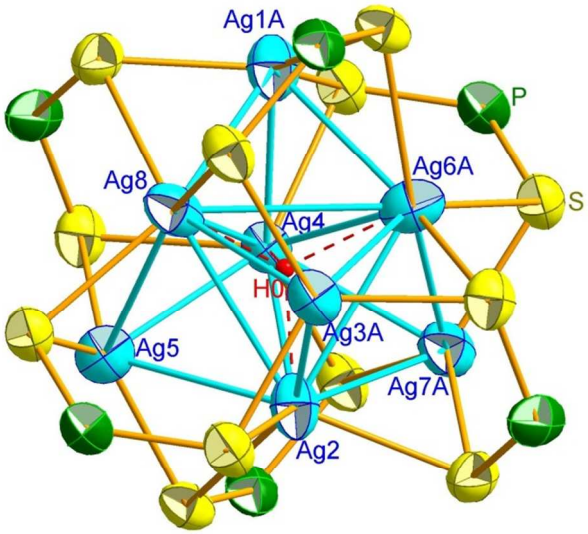

Fig. 4 Thermal ellipsoid drawing (50% probability) of the cluster $[Ag_8(\mu_4\text{-}H)\{S_2P(O^iPr)_2\}_6](PF_6)$, **5.** Only essential framework Ag/S/P/H atoms are shown for clarity.

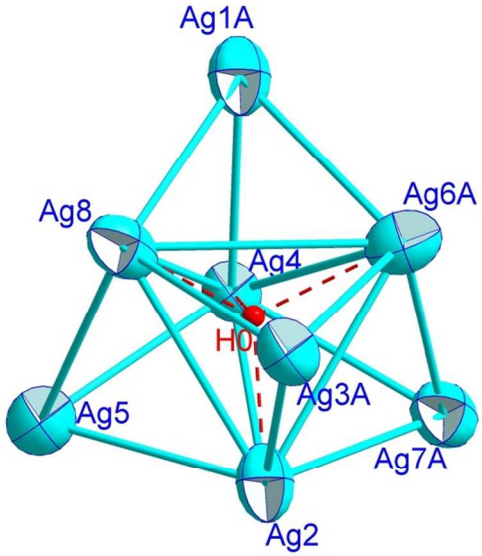

Fig. 5 Thermal ellipsoid drawing (50% probability) of the Ag_8H core for **5**. Symm. Code A: 0.5-x, 1.5-y, -z.

disordered.[31,32] For **5**, the eight silver atoms, stabilized inside the S_{12} icosahedron from six ligands, form a tetracapped tetrahedron with an interstitial hydride which is not located on the crystallographic center of inversion. A C_3 rotational axis passing through the vertex of the tetrahedron, the central hydride, and a capping Ag atom opposite the vertex, together with three C_2 axes each being co-linear with two opposite P atoms, constitute an idealized T symmetry for the cluster cation in **5**. The tetrahedronis constituted from the Ag2, Ag4, Ag8 and Ag6A atoms (abbr. as Ag_v) and each face of the tetrahedron is capped by Ag1A, Ag3A, Ag5 and Ag7A (abbr. as Ag_{cap}). The average edge length of the tetrahedron (Ag_v–Ag_v) 3.254 Å, is larger than Ag_v-Ag_{cap} [2.919 Å (av)], which are shorter than the sum of the van der Waals radii of two Ag atoms (3.4 Å).[30] Six dtp ligands, each of them retaining a tetrametallic, tetraconnective bonding mode, are located on the top of Ag_4 butterflies where hinge positions are edges of the tetrahedron and wingtips are two

Table 3 Selected bond distances (Å) and angles (deg) for **4** and **5** with e.s.d.s. in parentheses.

Complex **4**			
Ag(1)–S(1)	2.552(2)	P(1)–S(2)	2.018(4)
Ag(1)–S(3)	2.522(2)	P(2)–S(3)	2.021(3)
Ag(1)–S(5)	2.541(2)	P(2)–S(4)	2.010(3)
Ag(2)–S(1)	2.520(2)	P(3)–S(5)	2.013(4)
Ag(2)–S(4)	2.535(2)	P(3)–S(6)	2.008(3)
Ag(2)–S(6)	2.528(2)	Br(1)–Ag(1)	2.8839(9)
Ag(3)–S(2)	2.537(2)	Br(1)–Ag(2)	2.9449(9)
Ag(3)–S(3)	2.522(2)	Br(1)–Ag(3)	2.911(1)
Ag(3)–S(6)	2.528(3)	Br(1)–Ag(4)	2.9674(7)
Ag(4)–S(2)	2.520(2)	S(1)–P(1)–S(2)	121.5(1)
Ag(4)–S(4)	2.533(2)	S(3)–P(2)–S(4)	122.3(1)
Ag(4)–S(5)	2.511(3)	S(5)–P(3)–S(6)	123.0(2)
P(1)–S(1)	2.014(2)		
Complex **5**			
Ag(1A)–S(2)	2.472(2)	Ag(6A)–S(5A)	2.651(3)
Ag(1A)–S(3A)	2.483(2)	Ag(7A)–S(2A)	2.473(2)
Ag(1A)–S(6A)	2.458(2)	Ag(7A)–S(4)	2.471(2)
Ag(2)–S(2A)	2.667(3)	Ag(7A)–S(5A)	2.452(2)
Ag(2)–S(3)	2.654(3)	Ag(8)–S(2)	2.656(2)
Ag(2)–S(6)	2.673(3)	Ag(8)–S(4A)	2.658(3)
Ag(3A)–S(1A)	2.446(2)	Ag(8)–S(5)	2.675(3)
Ag(3A)–S(4A)	2.429(2)	P(1)–S(1)	1.987(3)
Ag(3A)–S(6)	2.437(2)	P(1)–S(2)	2.008(2)
Ag(4)–S(1)	2.681(3)	P(2)–S(3)	1.992(2)
Ag(4)–S(4)	2.685(2)	P(2)–S(4)	2.009(2)
Ag(4)–S(6A)	2.650(2)	P(3)–S(5)	2.010(2)
Ag(5)–S(1)	2.466(2)	P(3)–S(6)	2.002(2)
Ag(5)–S(3)	2.469(2)	S(1)–P(1)–S(2)	121.6(1)
Ag(5)–S(5)	2.462(2)	S(3)–P(2)–S(4)	121.8(1)
Ag(6A)–S(1A)	2.656(2)	S(5)–P(3)–S(6)	121.1(1)
Ag(6A)–S(3A)	2.630(3)		

Symmetric code: A: 0.5-x, 1.5-y, z

capping Ag atoms (Figure 4). The average dihedral angle observed in the Ag_4 butterflies of **5** is about 155°.

The Ag_v–S distances in **5** (av. 2.661 Å) are longer than Ag_{cap}–S (av. 2.460 Å) but remain in the normal range; however, the averaged S···S bite distance in **5** (3.492 Å) is comparable to the Cu homolog $[Cu_8(H)\{S_2P(O^iPr)_2\}_6]^+$.[32]

The hydride ion was located in the difference Fourier map, which is located at the tetrahedral hole and coordinated to four adjacent Ag atoms, (Fig. 5).

The averaged Ag-μ_4-H distance, 1.99(2) Å, is much longer than 1.831(5) Å that is observed in $[(PEt_3)_2(C_6Cl_5)Pt(\mu\text{-}H)Ag(H_2O)]^+$,[33] and the sum of the covalent radii (1.76(5) Å).

Cluster **5** contains only a single PF_6^- as a counter anion which supports the charge of the cluster being +1. Thus, with the support of NMR data and the symmetry consideration, the hydride is placed in the centre of Ag_4 tetrahedron.

Complex **6** crystallize in the monoclinic space group C2/c. Selected bond lengths and angles are presented in Table 4. A perspective view of cluster **6** is shown in Fig. 6. The X-ray structure reveals that the Ag_8 skeleton is in a cubic geometry with a sulfide anion entrapped in the centre. The coordination mode of each dtp ligand is a tetrametallic-tetraconnective (μ_2, μ_2) pattern, which is same as clusters **2** and **4**. The cluster contains an inversion center, three C_3 rotational axes pass through the body diagonal of the cube, and three C_2 rotational axes pass through the opposite P atoms to maintain an idealized T_h point group symmetry. No anions can be found in the lattice, indicating the

Dalton Transactions Accepted Manuscript

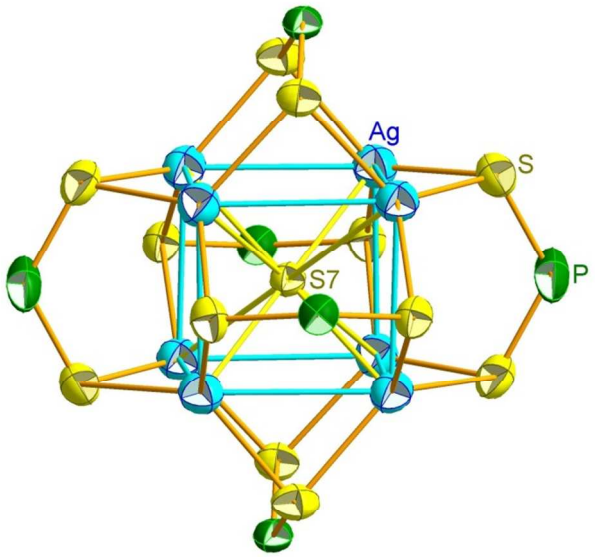

Fig. 6 Thermal ellipsoid drawing (50% probability) of $[Ag_8(\mu_8\text{-}S)\{S_2P(O^iPr)_2\}_6]$, **6**. Only the core framework atoms Ag/S/P and encapsulated S are shown for clarity.

Table 4 Selected bond distances (Å) and angles (deg) for **6** with e.s.d.s. in parentheses.

Ag(1)–S(1)	2.513(1)	P(1)–S(4)	1.999(2)
Ag(1)–S(4)	2.517(1)	P(2)–S(5)	2.012(2)
Ag(1)–S(6)	2.522(1)	P(2)–S(6)	2.008(2)
Ag(2)–S(2)	2.511(1)	P(3)–S(1)	2.010(1)
Ag(2)–S(3)	2.501(2)	P(3)–S(2)	2.014(2)
Ag(2)–S(6)	2.522(1)	S(7)–Ag(1)	2.8903(5)
Ag(3)–S(2)	2.520(1)	S(7)–Ag(2)	2.9151(3)
Ag(3)–S(4)	2.517(2)	S(7)–Ag(3)	2.8630(5)
Ag(3)–S(5)	2.522(1)	S(7)–Ag(4)	2.8327(5)
Ag(4)–S(1)	2.534(1)	S(3)–P(1)–S(4)	122.8(1)
Ag(4)–S(3)	2.531(1)	S(5)–P(2)–S(6)	122.19(8)
Ag(4)–S(5)	2.514(2)	S(1)–P(3)–S(2)	121.41(8)
P(1)–S(3)	2.005(2)		

neutral cluster must entrap an anion with -2 charge, as expected. The ligand "bite" distances of 3.509(2) ~ 3.519(2) Å and Ag–S bond lengths are in the range 2.501(2) to 2.534(1) Å. The Ag···Ag edge distances are in the range 3.2677(6) to 3.3901(6) Å (avg. in 3.3204 Å). The average Ag–S7 distance is 2.875 Å. Such Ag···Ag distances are in the range between those in complex **2** (av. 3.149 Å) and **4** (av. 3.380 Å), which is in agreement with the size effect of the entrapped anion. In comparison with the ethyl homolog $[Ag_8(S)\{S_2P(OEt)_2\}_6]$,[34] the Ag···Ag edge distances are in the range 3.228(4) to 3.495(6) Å (avg. in 3.361 Å), and the distance between Ag and central S atom is 2.780(4) Å. The distances in $[Ag_8(S)\{S_2P(OEt)_2\}_6]$ are in similar range but more distorted in the Ag_8 cube compared to complex **6**.

Complex **7**, $[Ag_{10}(\mu_9\text{-}I)(\mu_3\text{-}I)_3\{S_2P(O^iPr)_2\}_6]$, crystallize in the monoclinic space group P2(1)/n. Selected bond lengths and angles are presented in Table 5. A perspective view of cluster **7** is shown in Fig. 7 and a different perspective of the $Ag_{10}I$ core shown in Fig. 8. The X-ray structure reveals that the $Ag_{10}I$ core in **7** is analogous to the $Ag_{11}I$ core in $[Ag_{11}(\mu_9\text{-}I)(\mu_3\text{-}I)_3\{S_2P(O^iPr)_2\}_6]PF_6$,[22] the latter revealed a pentacapped trigonal prismatic geometry with an iodide entrapped in the centre. The Ag_{10} cage can be described as one Ag atom removed from the vertex of trigonal prism in Ag_{11}. The five atoms Ag1, Ag4, Ag2 Ag5, and Ag7 occupy the vertices of imperfect trigonal prism and

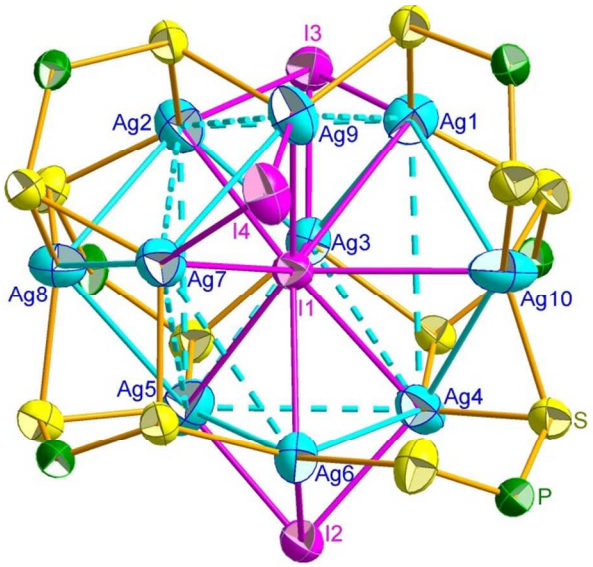

Fig. 7 Thermal ellipsoid drawing (50% probability) of $[Ag_{10}(\mu_9\text{-}I)(\mu_3\text{-}I)_3\{S_2P(O^iPr)_2\}_6]$, **7.** Only the core framework atoms Ag/S/P/I atoms are shown for clarity.

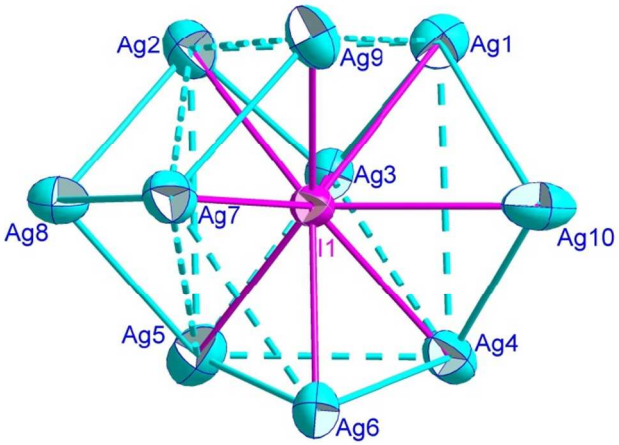

Fig. 8 Thermal ellipsoid drawing (50% probability) of the $Ag_{10}(\mu_9\text{-}I)$ core for **7.**

the capping Ag atoms (Ag3, Ag6, Ag8, Ag9, and Ag10) remain in the same positions. Four Ag4 butterflies are each capped by a dtp ligand in a tetrametallic tetraconnective (μ_2, μ_2) coordination pattern, where the other two ligands were each connected to two sets of three Ag atoms (Ag1, Ag9, Ag10, and Ag4, Ag6, Ag10) in a trimetallic triconnective (μ_2, μ_1) coordination pattern. The Ag–S distances are in the range of 2.455(2) – 2.695(2) Å, where the μ_1-S3–Ag10 and μ_1-S8–Ag6 distances are 2.455(2) and 2.493(2) Å, shorter than other μ_2-S–Ag distances. The μ_9-I–Ag distance is in the range of 3.1294(8) – 3.3501(8) Å, which are longer than the capping iodide to Ag distance which are in the range of 2.7118(7) – 2.8299(7) Å. Compared with the structure of $[Ag_{11}(\mu_9\text{-}I)(\mu_3\text{-}I)_3\{S_2P(O^iPr)_2\}_6]PF_6$, the μ_9-I–Ag distances are in the range of 3.1294(8) – 3.3501(8) Å and the μ_3-I–Ag distances are in the range of 2.7118(7) – 2.8299(7) Å. Both complexes reveal similar range in Ag–I distances.

Interestingly, further addition of $[Ag(CH_3CN)_4]PF_6$ to $[Ag_{10}(\mu_9\text{-}I)(\mu_3\text{-}I)_3\{S_2P(O^iPr)_2\}_6]$ (1:1 molar ratio) formed the cluster $[Ag_{11}(\mu_9\text{-}I)(\mu_3\text{-}I)_3\{S_2P(O^iPr)_2\}_6]PF_6$. By monitoring the ^{31}P NMR spectrum (Figure S21), a peak that resonate at 105.8 ppm and

Dalton Transactions Accepted Manuscript

This journal is © The Royal Society of Chemistry [year]

assigned to the Ag_{10} cluster vanished, and instead a new peak that

Table 5 Selected bond distances (Å) and angles (deg) for 7 with e.s.d.s. in parentheses.

Ag(1)–S(4)	2.503(1)	P(4)–S(8)	1.974(2)
Ag(1)–S(12)	2.508(2)	P(5)–S(9)	2.022(2)
Ag(2)–S(2)	2.503(1)	P(5)–S(10)	1.993(2)
Ag(2)–S(9)	2.510(2)	P(6)–S(11)	1.999(2)
Ag(3)–S(10)	2.526(2)	P(6)–S(12)	1.997(2)
Ag(3)–S(11)	2.515(1)	I(1)–Ag(1)	3.2319(6)
Ag(4)–S(7)	2.484(2)	I(1)–Ag(2)	3.3169(7)
Ag(4)–S(11)	2.506(1)	I(1)–Ag(3)	3.1648(8)
Ag(5)–S(6)	2.508(2)	I(1)–Ag(4)	3.2444(6)
Ag(5)–S(10)	2.523(2)	I(1)–Ag(5)	3.1296(8)
Ag(6)–S(5)	2.577(2)	I(1)–Ag(6)	3.1867(7)
Ag(6)–S(8)	2.493(2)	I(1)–Ag(7)	3.2254(6)
Ag(7)–S(1)	2.541(1)	I(1)–Ag(9)	3.1734(6)
Ag(7)–S(5)	2.573(2)	I(1)–Ag(10)	3.3501(8)
Ag(8)–S(1)	2.492(1)	I(2)–Ag(4)	2.8059(6)
Ag(8)–S(6)	2.497(2)	I(2)–Ag(5)	2.8011(8)
Ag(8)–S(9)	2.510(2)	I(2)–Ag(6)	2.8302(7)
Ag(9)–S(2)	2.695(2)	I(3)–Ag(1)	2.8171(7)
Ag(9)–S(4)	2.519(2)	I(3)–Ag(2)	2.7876(6)
Ag(10)–S(3)	2.456(2)	I(3)–Ag(3)	2.7505(7)
Ag(10)–S(7)	2.516(2)	I(4)–Ag(7)	2.7276(7)
Ag(10)–S(12)	2.626(2)	I(4)–Ag(9)	2.7118(7)
P(1)–S(1)	2.009(2)	S(1)–P(1)–S(2)	118.81(8)
P(1)–S(2)	2.003(2)	S(3)–P(2)–S(4)	118.08(9)
P(2)–S(3)	1.982(2)	S(5)–P(3)–S(6)	119.15(9)
P(2)–S(4)	2.019(2)	S(7)–P(4)–S(8)	118.3(1)
P(3)–S(5)	1.995(2)	S(9)–P(5)–S(10)	121.44(9)
P(3)–S(6)	2.017(2)	S(11)–P(6)–S(12)	121.22(9)
P(4)–S(7)	2.017(2)		

resonate at 103.2 ppm and assigned to the Ag_{11} cluster, formed. The time taken for the complete conversion was within 15 minutes. In addition, the methylene proton in Ag_{10} displayed a multiplet resonance at 4.91 ppm at the start. When the reaction was over, the presence of two chemical shifts for the methylene protons in the ^{1}H NMR spectrum clearly suggested the formation of Ag_{11}, which is due to the lack of a 2-fold rotational axis imposed on the dithiophosphato ligand. The structure of $[Ag_{10}(\mu_9\text{-}I)(\mu_3\text{-}I)_3\{S_2P(O^iPr)_2\}_6]$ displays an empty site which can coordinate an additional Ag ion and become an eleven-metal cluster, it could also potentially lead to a heterometallic cluster by adding one equivalent of a different metal salt, ie Au ion.

Conclusions

The present study demonstrates that mono- and dianionic (and thus far) monoatomic species can be efficiently encapsulated within a Ag_8 core as well as in higher nuclearity silver(I)/sulfur systems. This is proposed to include a polymeric Ag_5 precursor material which readily converts to Ag_8 clusters in solution and in the presence of a suitable anion templating agent. We further propose that these clusters form through rational design principles (as opposed to relying on serendipitous outcomes) since the M:L:X ratio used correspond to the formula stoichiometry of the final products in all cases. Further work in this area would expand to encapsulate small di- or triatomic anions (CN^-, OH^-,OCl^- OCN^-, NO_2^- etc.) within the structures.

Acknowledgements

Financial supports from the Ministry of Science and Technology in Taiwan (NSC 100-2113-M-259-003-MY3) are gratefully acknowledged.

References

1 J. L. Sessler, P. A. Gale and W.-S. Cho, *Anion Receptor Chemistry*, RSC, Cambridge, 2006.
2 P. D. Beer and P. A. Gale, *Angew. Chem. Int. Ed.* 2001, **40**, 486.
3 J. M. Llinares, D. Powell and K. Bowman-James, *Coord. Chem. Rev*. 2003, **240**, 57.
4 E. J. O'Neil and B. D. Smith, *Coord. Chem. Rev*. 2006, **250**, 3068.
5 R. Martínez-Manez and F. Sancenón, *Coord. Chem. Rev*. 2006, **250**, 3081.
6 T. Gunnlaugsson, M. Glynn, G. M. Tocci, P. E. Kruger and F. M. Pfeffer, *Coord. Chem. Rev*. 2006, **250**, 3094.
7 C. R. Rice, *Coord. Chem. Rev*. 2006, **250**, 3190.
8 P. A. Gale, S. E. García-Garrido and J. Garric, *Chem. Soc. Rev*. 2008, **37**, 151.
9 J. Pérez and L. Riera, *Chem. Soc. Rev*. 2008, **37**, 2658.
10 J. W. Steed, *Chem. Soc. Rev*. 2009, **38**, 506.
11 Y. Hua and A. H. Flood, *Chem. Soc. Rev*. 2010, **39**, 1262.
12 A. Caballero, F. Zapata and P. D. Beer, *Coord. Chem. Rev*. 2013, **257**, 2343.
13 K. Worm and F. P. Schmidtchen, *Angew. Chem. Int. Ed. Engl*. 1995, **34**, 65.
14 P. B. Savage, S. K. Holmgren and S. H. Gellman, *J. Am. Chem. Soc*. 1994, **116**, 4069.
15 M. W. Hosseini and J.-M. Lehn, *J. Am. Chem. Soc*. 1982, **104**, 3525.
16 (a) M. O. Awaleh, A. Badia and F. Brisse, *Cryst. Growth Des*. 2005, **5**, 1897; (b) K. Tang, M. Aslam, E. Block, T. Nicholson and J. Zubieta, *Inorg. Chem*. 1987, **26**, 1488; (c) H. Brunner, A. Hollman, M. Zabel and B. Nuber, *J. Organomet. Chem.* 2000, 609, 44; (d) S. Wang, J. P. Fackler, Jr. and T. F. Carlson, *Organometallics*, 1990, **9**, 1973.
17 (a) X. Jin, X. Xie, H. Qian, K. Tang, C. Liu, X. Wang and Q. Gong, *Chem. Commun*., 2002, 600; (b) K. Tang, J. Yang, Q. Yang and Y. Tang, *J. Chem. Soc., Dalton Trans*., 1989, 2297; (c) C. W. Liu, J. T. Pitts and J. P. Fackler, Jr., *Polyhedron*, 1997, **16**, 3899; (d) M. Shi, J.-K. Jiang and G.-L. Zhao, *Eur. J. Inorg. Chem*., 2002, 3264; (e) W. E. van Zyl, *Comments Inorg. Chem*., 2010, **31**, 13; (f) W. E. van Zyl and J. D. Woollins, *Coord. Chem. Rev*. 2013, **257**, 718.
18 (a) X. Jin, K. Tang, W. Liu, H. Zeng, H. Zhao, Y. Ouyang and Y. Tang, *Polyhedron*, 1996, **15**, 1207; (b) W. Shi, R. Ahlrichs, C. E. Anson, A. Rothenberger, C. Schrodt and M. Shafaei-Fallah, *Chem. Commun*., 2005, 5893.
19 (a) P. D. Beer and S. R. Bayly, *Topics in Current Chemistry* vol. 255, Springer, Berlin, 2005, pp. 125–162; (b) G. H. Reeu and M. Cohn, *J. Biol. Chem*., 1972, **247**, 3073; (c) D. Rais, D. M. P. Mingos, R. Vilar, A. P. J. White and D. J. Williams, *J. Organomet. Chem*., 2002, **652**, 87; (d) Y.-P. Xie and T. C. W. Mak, *J. Cluster Sci*., 2014, **25**, 189.
20 (a) C. W. Liu, I.-J. Shang, J.-C. Wang and T.-C. Keng, *Chem. Commun.,* 1999, 995; (b) C. W. Liu, I.-J. Shang, C.-M. Hung, J.-C. Wang and T.-C. Keng, *J. Chem. Soc., Dalton Trans*., 2002, 1974; (c) C. W. Liu, H.-C. Haia, C.-M. Hung, B. K. Santra, B.-J. Liaw, Z. Lin and J.-C. Wang, *Inorg. Chem*. 2004, **43**, 4464; (d) C. Latouche, C. W. Liu and J.-Y. Saillard, *J. Cluster Sci*., 2014, **25**, 147.
21 C. W. Liu, H.-W. Chang, C.-S. Fang, B. Sarkar and J.-C. Wang, *Chem. Commun*., 2010, **46**, 4571.
22 Y.-J. Li, C. Latouche, S. Kahlal, J.-H. Liao, R. S. Dhayal, J.-Y. Saillard and C. W. Liu, *Inorg. Chem*. 2012, **51**, 7439.
23 D. D. Perrin, W. L. F. Armarego and D. R. Perrin, Purification of Laboratory Chemicals, Pergamon Press, Oxford, 2nd edn, 1980.
24 Wystrach, V. P.; Hook, E. O.; Christopher G. L. M. *J. Org. Chem.* 1956, **21**, 705-707.
25 Kubas, G. J. *Inorg. Synth*. 1979, **19**, 90-112.
26 *SAINT V4.043: Software for the CCD Detector System*; Bruker Analytical X-ray System: Madison, WI, 1995.
27 G. M. Sheldrick, *SADABS*; University of Gottingen: Gottingen, Germany, 1996.

Dalton Transactions Accepted Manuscript

28 SHELXL-97: G. M. Sheldrick, *Program for the Refinement of Crystal Structure*; University of Göttingen: Göttingen, Germany, 1997.
29 SHELXL 5.10 (PC version): *Program Library for Structure Solution and Molecular Graphics*; Bruker analytical X-ray System: Madison, WI, 1998.
30 J. E. Huheey, Inorganic Chemistry, Walter de Gruyter, Berlin, 1988. p. 278.
31 C. W. Liu, B. Sarkar, Y.-J. Huang, P.-K. Liao, J.-C. Wang, J.-Y. Saillard and S. Kahlal, *J. Am. Chem. Soc*. 2009, **133**, 11222.
32 P.-K. Liao, B. Sarkar, H.-W. Chang, J.-C. Wang and C. W. Liu, *Inorg. Chem.* 2009, **48**, 4089.
33 A. Albinati, S. Chaloupka, F. Demartin, T. F. Koetzle, H. Ruegger, L. M. Venanzi and M. K. Wolfer, *J. Am. Chem. Soc.* 1993, **115**, 169.
34 K. Matsumoto, R. Tanaka, R. Shimomura and Y. Nakao, *Inorg. Chim Acta*, 2000, **304**, 293.

Dalton Transactions Accepted Manuscript

This journal is © The Royal Society of Chemistry [year]

Table of Content

The polymer $[Ag_5\{S_2P(O^iPr)_2\}_4]_n(PF_6)_n$ forms discrete Ag_8 and Ag_{10} clusters with encapsulated anions; the nuclearity depends on the M:L stoichiometric control.

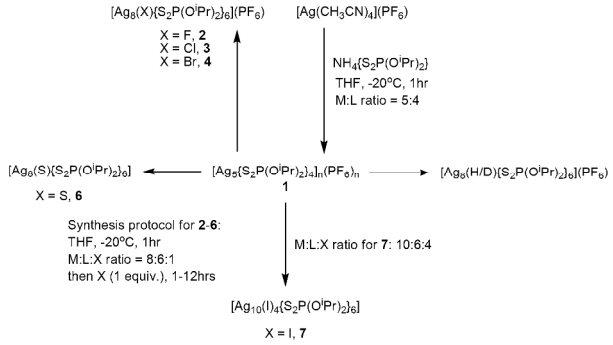

Dalton Transactions Accepted Manuscript